King, G. C., & Coleman, J. E. (1987) *Biochemistry 26*, 2929-2937.
King, G. C., & Coleman, J. E. (1988) *Biochemistry 27*, 6947-6953.
Means, G. E. (1977) *Methods Enzymol. 47*, 469-478.
Otto, C., de Mul, F. F. M., Harmsen, B. J. M., & Greve, J. (1987) *Nucleic Acids Res. 15*, 7605-7625.
Porschke, D., & Rauh, H. (1983) *Biochemistry 22*, 4737-4745.
Sherry, A. D., & Teherani, J. (1983) *J. Biol. Chem. 258*, 8663-8669.
Sherry, A. D., Geraldes, C. F. G. C., & Cacheris, W. P. (1987) *Inorg. Chim. Acta 139*, 137-139.
Sherry, A. D., Malloy, C. R., Jeffrey, F. M. H., Cacheris, W. P., & Geraldes, C. F. G. C. (1988) *J. Magn. Reson. 76*, 528-533.
Valentine, R. C., Shapiro, B. M., & Stadtman, E. R. (1968) *Biochemistry 7*, 2143-2152.
Williams, R. J. P., Moore, G. R., & Williams, G. (1984) in *Progress in Bioorganic Chemistry and Molecular Biology* (Ovchinnikov, Y. A., Ed.) pp 31-39, Elsevier, Amsterdam and New York.

Range of the Solvation Pressure between Lipid Membranes: Dependence on the Packing Density of Solvent Molecules†

Thomas J. McIntosh,*,‡ Alan D. Magid,‡ and Sidney A. Simon§
Departments of Cell Biology, Neurobiology, and Anesthesiology, Duke University Medical Center, Durham, North Carolina 27710

Received April 19, 1989; Revised Manuscript Received June 6, 1989

ABSTRACT: Well-ordered multilamellar arrays of liquid-crystalline phosphatidylcholine and equimolar phosphatidylcholine–cholesterol bilayers have been formed in the nonaqueous solvents formamide and 1,3-propanediol. The organization of these bilayers and the interactions between apposing bilayer surfaces have been investigated by X-ray diffraction analysis of liposomes compressed by applied osmotic pressures up to 6×10^7 dyn/cm^2 (60 atm). The structure of egg phosphatidylcholine (EPC) bilayers in these solvents is quite different than in water, with the bilayer thickness being largest in water, 3 Å narrower in formamide, and 6 Å narrower in 1,3-propanediol. The incorporation of equimolar cholesterol increases the thickness of EPC bilayers immersed in each solvent, by over 10 Å in the case of 1,3-propanediol. The osmotic pressures of various concentrations of the neutral polymer poly(vinylpyrrolidone) dissolved in formamide or 1,3-propanediol have been measured with a custom-built membrane osmometer. These measurements are used to obtain the distance dependence of the repulsive solvation pressure between apposing bilayer surfaces. For each solvent, the solvation pressure decreases exponentially with distance between bilayer surfaces. However, for both EPC and EPC–cholesterol bilayers, the decay length and magnitude of this repulsive pressure strongly depend on the solvent. The decay length for EPC bilayers in water, formamide, and 1,3-propanediol is found to be 1.7, 2.4, and 2.6 Å, respectively, whereas the decay length for equimolar EPC–cholesterol bilayers in water, formamide, and 1,3-propanediol is found to be 2.1, 2.9, and 3.1 Å, respectively. These data indicate that the decay length is inversely proportional to the cube root of the number of solvent molecules per unit volume. Thus, the decay length of the solvation pressure depends on the packing of the solvent molecules in the interbilayer space but is not strongly dependent on either the solvent's dielectric constant or the dipole moment. The magnitude of the solvation pressure, which is largest in water and smallest in 1,3-propanediol, varies with the square of the dipole potential as measured in monolayers in equilibrium with bilayers.

To bring two polar surfaces together, one must remove the intervening solvent molecules. Because the solvent molecules are ordered by the surfaces, the removal of these molecules requires energy and gives rises to a large, short-range repulsive pressure, called the solvation pressure, P_{sol}, or, if the solvent is water, the hydration pressure, P_h. For several polar and nonpolar solvents, including water, cyclohexane, and octane, Israelachvili and colleagues (Christenson et al., 1982; Israelachvili & Pashley, 1983; Israelachvili, 1985) have shown that the solvation pressure between smooth solid surfaces such as mica sheets, while overall repulsive, is an oscillatory function of the fluid spacing between the mica sheets. They found that the distance between successive minima in P_{sol} corresponds approximately to the diameter of the solvent molecule. For surfaces which are "micro-rough" or fluid, such as biological membranes and lipid bilayers, these oscillations are smeared out and the solvation pressure decreases monotonically with distance (Israelachvili & Pashley, 1983; Rand et al., 1979).

For lipid bilayers with water as the solvent, P_h has been quantitated by X-ray diffraction measurements of multilayers squeezed together by osmotic pressure. For several types of lipid bilayers immersed in water, it has been found that P_h decays exponentially with distance between bilayers (d_f) such that $P_h = P_0 \exp(-d_f/\lambda)$, where the decay length λ is on the order of 1–2 Å (LeNeveu et al., 1977; Parsegian et al., 1979; Lis et al., 1982; McIntosh & Simon, 1986; Simon et al., 1988).

Less work has been done on the solvation pressure between bilayers in liquids other than water, although a number of studies have shown that multilamellar phosphatidylcholine liposomes can be formed in nonaqueous solvents. These sol-

† Supported by NIH Grant GM-27278.
‡ Department of Cell Biology.
§ Departments of Neurobiology and Anesthesiology.

0006-2960/89/0428-7904$01.50/0

Table I: Physical Properties of Solvents

	solvent				
	water	formamide	1,3-propanediol	1,2-propanediol	glycerol
M_w (g/mol)	18	45.05	76.11	76.11	92
density (g/cm^3)	0.998[a]	1.133[a]	1.059[a]	1.036[a]	1.2613[a]
molecular volume (Å^3)	30	66	119	119	121
molecular density, n_s (Å^{-3})	0.033	0.0151	0.0084	0.0084	0.0083
dipole moment (D)	1.85[b]	3.73[b]	2.50[a]	2.75[a]	2.56[b]
surface tension (dyn/cm)	72.75[a]	57.44[b]	45.62[b]	35.5[c]	63.4[a]
dielectric constant, ϵ	78.3[a]	111.0[a]	35[a]	32.0[a]	42.5[a]
index of refraction, n	1.33299[b]	1.4472[b]	1.4398[b]	1.4324[b]	1.4746[b]
area/molecule of EPC (Å^2)	64[e]	70[e]	76[e]	(d)[e]	68[e]

[a] Dean, 1985. [b] *Handbook of Chemistry and Physics*, 66th Edition. [c] Nakanishi et al., 1971. [d] Does not form lamellar phase. [e] This study.

vents include dipolar liquids such as ethylene glycol (McDaniel et al., 1983; Persson & Bergenstahl, 1985), glycerol (McDaniel et al., 1983), and formamide (Bergenstahl & Stenius, 1987), saccharides such as trehalose (Crowe & Crowe, 1988), and the fused salt, ethylammonium nitrate (Evans et al., 1983). For instance, Bergenstahl and Stenius (1987) obtained phase diagrams for egg phosphatidylcholine (EPC) in formamide, methyl formamide, and dimethylformamide. They showed that a necessary, but not sufficient, condition for solvents to swell lipid multilayers is that they must form hydrogen bonds with the lipid. They also noted that the ability to "solvate" the EPC headgroup is not related in a simple way to the solvent's dielectric constant, dipole moment, or index of refraction. For lipid bilayers, P_{sol} has been measured in one nonaqueous solvent, ethylene glycol (Persson & Bergenstahl, 1985). On the basis of repulsive pressure versus distance data obtained from vapor pressure measurements, Persson and Bergenstahl (1985) have suggested that the decay length of P_{sol} for lecithin bilayers is similar in ethylene glycol and in water.

There have been several theoretical treatments of the solvation pressure (Marcelja & Radic, 1976; Schiby & Ruckenstein, 1983; Gruen & Marcelja, 1983; Jonsson & Wennerstrom, 1983; Cevc & Marsh, 1985; Graham et al., 1986; Belaya et al., 1986; Kornyshev, 1986; Dzhavakhidze et al., 1986). However, at this time there is not general agreement as to how the magnitude and decay length of P_{sol} should depend on the properties of the solvent molecules. For example, it has been suggested that the decay length of P_{sol} should depend on the solvent's static or optical dielectric constants (Gruen & Marcelja, 1983), number and type of hydrogen-bonding defects in the solvent (Attard & Batchelor, 1988), and size of the solvent molecule (Schiby & Ruckenstein, 1983).

In this paper, we investigate for lipid bilayers how both the magnitude and decay length of P_{sol} depend on the properties of the solvent molecule. By the use of X-ray diffraction analysis of osmotically stressed phosphatidylcholine and phosphatidylcholine–cholesterol multilayers, we measure P_{sol} as a function of distance for two nonaqueous solvents, formamide and 1,3-propanediol, whose dimensions, as well as several other physical properties, are quite different than those of water (Table I).

Materials and Methods

Egg phosphatidylcholine (EPC)[1] was obtained from Avanti Polar Lipids, Inc., and cholesterol (99+%) was obtained from Sigma Chemical Co. Both lipids were used without further purification. Poly(vinylpyrrolidone) (PVP) with an average molecular weight of 40 000 and formamide were obtained from Sigma Chemical Co., glycerol and 1,3-propanediol (referred to in this paper as 1,3-PDO) were obtained from Aldrich, and 1,2-propanediol was purchased from Fisher.

Osmotic pressures were applied to unoriented lipid suspensions in either formamide or 1,3-PDO by the "osmotic stress" procedures developed by Parsegian, Rand, and colleagues (LeNeveu et al., 1977; Parsegian et al., 1986) and previously applied to aqueous suspensions of lipids (LeNeveu et al., 1977; Parsegian et al., 1979; McIntosh & Simon, 1986; McIntosh et al., 1989a). EPC or EPC–cholesterol mixtures were rotary evaporated from chloroform, and an excess amount (greater than 80% by weight) of the appropriate PVP/formamide or PVP/1,3-PDO solution was added. The suspensions were covered with dry nitrogen and incubated for several hours with periodic vortexing. An excess fluid phase was always observed by examination of the specimens with a light microscope equipped with crossed polarizers. Because PVP is too large to enter between the lipid multilayers, it competes for solvent with the lipid and therefore compresses the lamellar lattice (LeNeveu et al., 1977; Parsegian et al., 1979).

For X-ray diffraction experiments, the lipid suspensions were sealed in quartz glass capillary tubes and mounted in a point-collimation X-ray camera. For gravimetric analysis (see below), carefully weighed lipid–solvent mixtures were allowed to incubate several hours under nitrogen, sealed in capillary tubes, and mounted in the same point-collimation camera. Oriented specimens of EPC in formamide or 1,3-PDO were made by the following procedure. A small drop of EPC dissolved in chloroform was placed on a narrow strip of aluminum foil and allowed to dry. A droplet of PVP dissolved in either formamide or 1,3-PDO was applied to the spot of lipid. The aluminum foil substrate was given a convex curvature, covered with a strip of polyethylene film that acted to hold a thin layer of the PVP/solvent solution in contact with the EPC multilayers, and placed in a chamber kept at low relative humidity by a flow of dry nitrogen. The specimen was mounted on a line-focused single-mirror X-ray camera so that the X-ray beam was oriented at a grazing angle relative to the oriented multilayers. The aluminum foil–polyethylene sandwich contacted a reservoir of PVP–solvent solution at one edge so as to retain the layer of PVP solution during the X-ray exposure. Such specimens gave four to five diffraction orders in contrast to the three orders that bulk suspensions of EPC multilamellar liposomes in the same solvents typically gave. For EPC–cholesterol multilayers, four or five orders were obtained with bulk suspensions, so that oriented specimens were not used.

For all specimens, oriented multilayers and unoriented lipid–polymer–solvent and lipid–solvent suspensions, X-ray diffraction patterns were recorded on Kodak DEF X-ray film. X-rays were obtained from a Jarrell-Ash microfocus X-ray

[1] Abbreviations: PVP, poly(vinylpyrrolidone); 1,3-PDO, 1,3-propanediol; EPC, egg phosphatidylcholine; SOPC, 1-stearoyl-2-oleoylphosphatidylcholine.

generator. All patterns were recorded at 20 °C. Films were processed by standard techniques and densitometered with a Joyce-Loebl Model MKIIIC microdensitometer. For the unoriented specimens, the densitometer trace was taken in a radial direction from the center of the film, whereas for the oriented specimens the trace was taken through the center of each reflection. After background subtraction, integrated intensities, $I(h)$, were obtained for each order h by measuring the area under each diffraction peak. For unoriented patterns the structure amplitude $F(h)$ was set equal to $[h^2I(h)]^{1/2}$ (Blaurock & Worthington, 1966; Herbette et al., 1977). For the oriented line-focused patterns, there was no detectable arcing of the reflections, which were of uniform height. In this case, the intensities were corrected by a single factor of h due to the cylindrical curvature of the multilayers (Blaurock & Worthington, 1966; Herbette et al., 1977), so that $F(h) = [hI(h)]^{1/2}$. The validity of this correction factor for this specimen geometry has been demonstrated previously (McIntosh et al., 1987). In should also be noted that structure factors from oriented and unoriented EPC/PVP/solvent specimens fell on the same continuous transform, except that the data from the oriented multilayers extended to higher resolution ($d/2h_{max} \cong 5$ Å).

Estimates for the widths of the bilayer and solvent layer between adjacent bilayers were obtained from the X-ray diffraction data by two methods—calculation of electron density profiles and gravimetric analysis. Electron density profiles on a relative electron density scale were calculated from

$$\rho(x) = (2/d)\sum_h \exp[\phi(h)]\, F(h) \cos(2\pi xh/d) \quad (1)$$

where d is the lamellar repeat period and $\phi(h)$ is the phase angle for each order h. Phase angles were determined from a sampling theorem analysis as described in detail previously (McIntosh & Holloway, 1987). All electron density profiles described in this paper were at a resolution of $d/2h_{max} = 5$–6 Å.

In the gravimetric analysis, the partial lipid thickness (d_l), partial thickness of the solvent layer (d_s), and the area per lipid molecule (A) were obtained following the method of Luzzati (1968). The partial lipid and solvent thicknesses and area per molecule were calculated from

$$d_l = [cv_l/[cv_l + (1 - c)v_s]]d \quad (2)$$

$$d_s = d - d_l \quad (3)$$

$$A = 2Mv_l/d_lN \quad (4)$$

where c is the weight fraction of lipid, v_l and v_s are the partial specific volumes of lipid and solvent, respectively, M is the molecular weight of the lipid, and N is Avogadro's number. In these calculations, v_l was set equal to 1 and the molecular weight of EPC was taken as 770. The partial specific volumes for water, formamide, and 1,3-PDO were taken as their values in bulk solution, namely, 1.000, 0.882, and 0.944 cm^3/g, respectively.

Osmotic pressures of PVP/water, PVP/formamide, and PVP/1,3-PDO solutions were measured with a custom-built membrane osmometer. Following the procedure of Vink (1971), we prepared PVP solutions gravimetrically (g/g) and converted to volumetric measure (g/mL) from measurements of the density of each solution. Details of the osmometer's design, fabrication, and operation will be presented elsewhere. Briefly, the osmometer consisted of a dialysis membrane clamped between two lucite blocks into which compartments for the sample and reference solutions had been milled. The side of the membrane that was exposed to the reference solution (lower osmotic pressure) was supported by a perforated stainless steel plate. Attached to the sample chamber was a modified commercial strain-gage pressure transducer (Columbia Research Labs) which generates a voltage proportional to pressure (1.0 V = 6.9 × 10^6 dyn/cm^2). Two kinds of membranes were used. For water and formamide solutions, a benzoylated cellulose membrane with a 2000 M_w exclusion limit (Sigma Chemical Co.) was employed. For 1,3-PDO solutions, a type C ultrafiltration membrane with a 1000 M_w exclusion limit (Spectrum Medical Industries, Los Angeles) was used because the cellulose membrane was only poorly permeable to 1,3-PDO. The pressure signal was recorded continuously until it did not change with time. The osmometer was held in a thermostated chamber at 20 ± 0.5 °C. Osmotic pressures were measured with pure solvent in the reference cell unless pressures higher than the limit of the pressure transducer were expected. In that case, the reference solution was a polymer solution at a suitably lower concentration.

For dipole potential measurements, monolayers were formed by spreading 10–40 μL of a lipid–chloroform solution (25 mg/mL) onto the appropriate solvent containing 1 mM KCl. A Teflon trough with a surface area of about 30 cm^2 was used, as described previously (MacDonald & Simon, 1987). To ensure that the surface was free of surface-active impurities, the KCl was roasted at 600 °C and the subphase was vacuum aspirated immediately before the monolayer was spread. The trough was emptied and thoroughly cleaned between runs. The dipole potential was measured between a Ag/AgCl electrode in the subphase and a polonium electrode in the air which was connected to a Keithly electrometer, Model 602. The reported values of dipole potential represent the difference in the potential of the subphase surface in the presence and absence of the monolayer.

Results

For EPC in glycerol, formamide, and 1,3-propanediol the X-ray diffraction patterns contain a series of low-angle reflections, which index as orders of a lamellar repeat period, and a broad wide-angle band with an average spacing of about 4.5 Å. These patterns are typical of bilayers in the liquid-crystalline phase (Tardieu et al., 1973). These specimens all are birefringent when viewed with a light microscope equipped with cross polarizers. In contrast, specimens of EPC in 1,2-propanediol give no sharp low-angle reflections and are non-birefringent. These observations indicate that multilamellar EPC liposomes form in glycerol, formamide, and 1,3-propanediol, but not in 1,2-propanediol. Unfortunately, glycerol could not be used in osmotic stress experiments because PVP is only sparingly soluble in glycerol, giving too narrow a pressure range. Therefore, osmotic stress experiments were performed only with formamide and 1,3-propanediol (1,3-PDO).

Osmotic pressure data for PVP in water, formamide, and 1,3-PDO are shown in Figure 1. The data for PVP/water solutions are similar to those published by Parsegian et al. (1986) and are in close agreement with pressures calculated by using the virial coefficients determined at lower pressures by Vink (1971). The pressure versus PVP concentration curves are almost identical for water and formamide. However, a given concentration of PVP in 1,3-PDO produces a higher osmotic pressure compared to PVP in water or formamide (Figure 1).

Plots of the natural logarithm of applied pressure (ln P) versus lamellar repeat period (d) for EPC in solutions of PVP in water, formamide, and 1,3-PDO are shown in Figure 2.

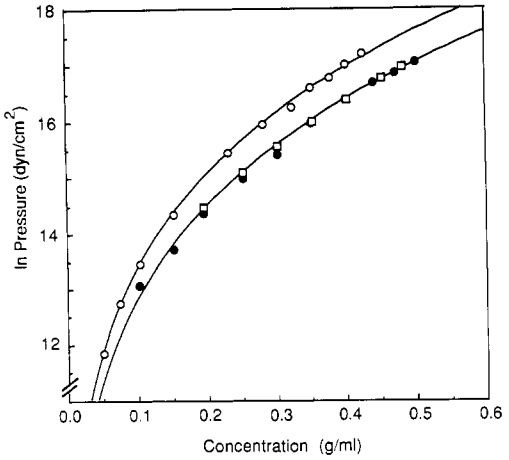

FIGURE 1: Measured osmotic pressure versus PVP concentration in water (□), formamide (●), and 1,3-propanediol (○).

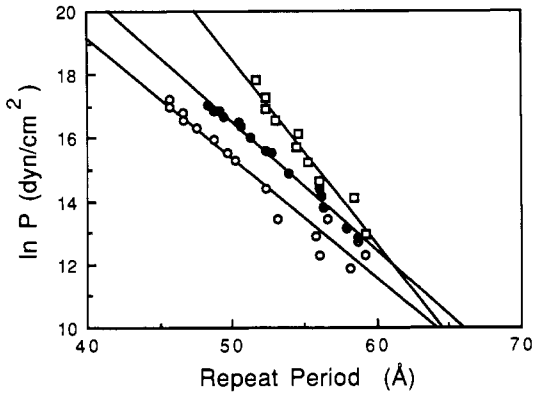

FIGURE 2: Natural logarithm of applied pressure versus lamellar repeat period for EPC multilayers in water (□) [from McIntosh and Simon (1986)], formamide (●), and 1,3-PDO (○).

Note that the data points for each solvent system fit closely to a straight line ($r^2 > 0.96$ for each regression).

In these diffraction experiments, each unit cell contains one bilayer and the fluid space between adjacent bilayers. That is, the lamellar repeat period (d) is comprised of the width of each bilayer (d_b) plus the width of each fluid space between adjacent bilayers (d_f). We have estimated d_b and d_f both from electron density profiles and from gravimetric data.

Panels A, B, and C of Figure 3 show typical electron density profiles for EPC in PVP/water, PVP/formamide, and PVP/1,3-PDO solutions, respectively. For each profile, the geometric center of the bilayer is at the origin (0 Å). The low-density regions in the center of each bilayer correspond to the lipid hydrocarbon chains, and the highest density peaks, located at about ±19 Å for EPC in PVP/water, ±17 Å for EPC in PVP/formamide, and ±16 Å for EPC in PVP/1,3-PDO, correspond to the lipid headgroups. The medium-density regions at the outer edges of each profile correspond to the fluid spaces between adjacent bilayers. Several observations can be made from these profiles. First, for each solvent the bilayer structure remains nearly the same for each PVP concentration. That is, the distance between headgroup peaks and the shape of the bilayer region of the profile stay approximately constant as adjacent bilayers are squeezed together by the osmotic pressure. Second, the fluid space between adjacent bilayers decreases with increasing PVP concentration. Third, the distance between headgroup peaks, d_{pp}, is largest in PVP/water and smallest in PVP/1,3-PDO (see Table II). Fourth, in PVP/water solutions, but not in PVP/formamide or PVP/1,3-PDO solutions, there is a distinct low-density dip

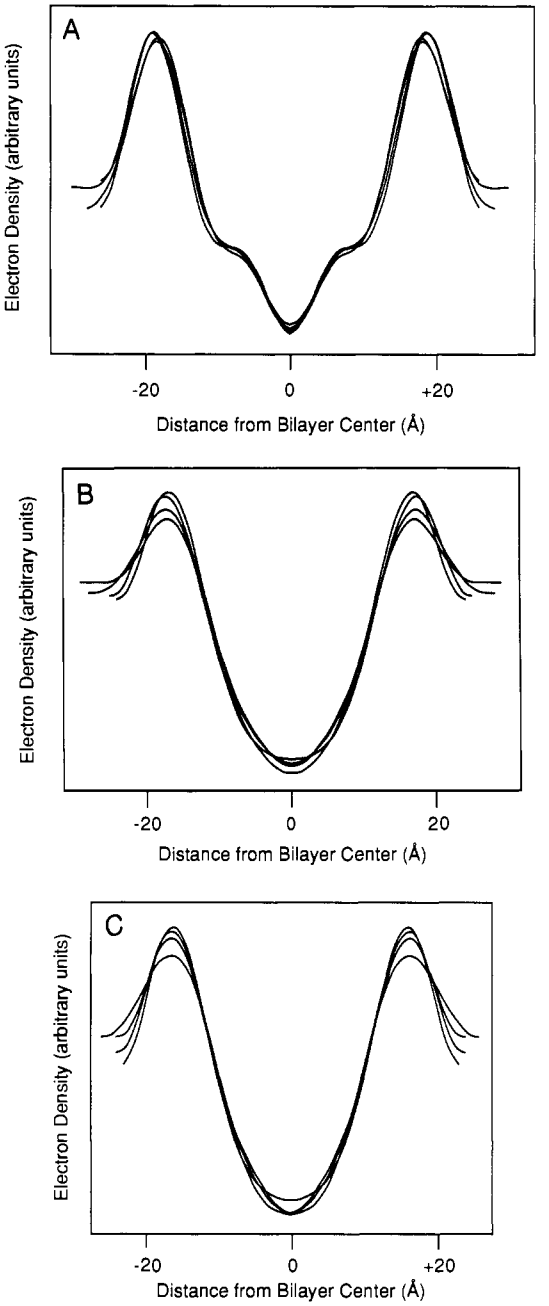

FIGURE 3: Electron density profiles for EPC in PVP solutions in (A) water [from McIntosh and Simon (1986)], (B) formamide, and (C) 1,3-PDO. The ranges of repeat periods shown are 51.7–63.2 Å for water, 49.1–57.8 Å for formamide, and 46.6–51.2 Å for 1,3-PDO.

Table II: Comparison of the Structure of EPC Bilayers As Obtained by Electron Density Profiles and Gravimetric Analysis

solvent	d_{pp} (electron density) (Å)	d_l (gravimetric) (Å)
water	37.8 ± 0.8 (N = 10)	39.9 ± 1.0 (N = 7)
formamide	34.0 ± 1.0 (N = 6)	36.5 ± 0.5 (N = 6)
1,3-PDO	31.6 ± 0.4 (N = 4)	33.8 ± 1.2 (N = 10)

or trough in the center of the bilayer. This trough corresponds to the localization of the low-density lipid terminal methyl groups in the center of the bilayer. The presence of this trough in profiles of EPC in water (Figure 3A) and its absence in formamide (Figure 3B) or 1,3-PDO (Figure 3C) imply that the hydrocarbon chains are more regularly ordered in bilayers in water than they are in bilayers in formamide or 1,3-PDO. This is consistent with the bilayer width being greater (and the area per molecule being smaller) in water than in form-

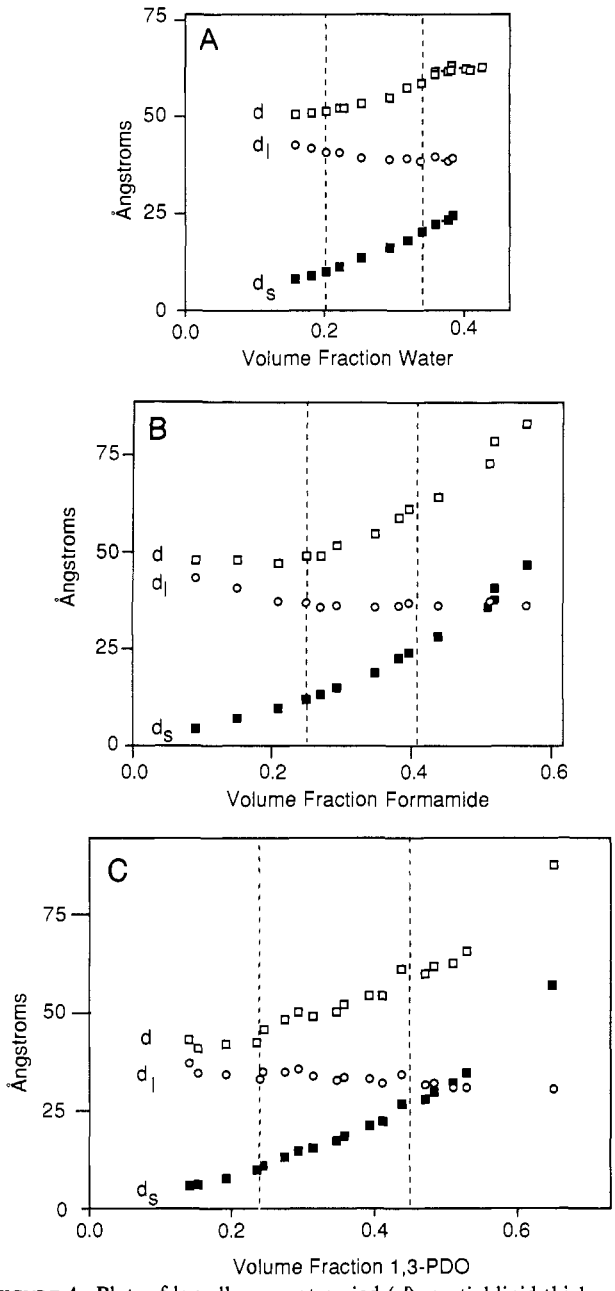

FIGURE 4: Plots of lamellar repeat period (d), partial lipid thickness (d_l), and partial solvent thickness (d_s) versus volume fraction solvent for EPC in (A) water, (B) formamide, and (C) 1,3-PDO.

amide or 1,3-PDO (Table II).

Plots of d, d_l (calculated from eq 2), and d_s (calculated from eq 3) versus volume fraction of solvent for EPC in water, formamide, and 1,3-PDO are shown in panels A, B, and C, respectively, of Figure 4. The swelling behavior of EPC is similar in each of these solvents, except at large volume fractions of solvent. The lamellar repeat period and partial fluid thickness increase monotonically with volume fraction solvent for EPC bilayers in formamide (Figure 4B) and 1,3-PDO (Figure 4C), as was previously observed for dioleoylphosphatidylcholine bilayers in formamide (Bergenstahl & Stenius, 1987). In contrast, in water the repeat period for EPC bilayers increases with increasing water content until a volume fraction of about 35%, whereupon the repeat period remains constant with further increases in water content [Figure 4A, Small (1967), and LeNeveu et al. (1977)]. In Figure 4, the pair of vertical dashed lines delimit the range of repeat periods recorded in the osmotic stress experiments (Figure 2). For each solvent the partial lipid thickness, d_l, remains approximately constant for this range of repeat periods. The average values for d_l for these repeat period ranges are given in Table II. Note that for each solvent the peak-to-peak distance, d_{pp}, as measured from the electron density profiles is 2–2.5 Å smaller than the partial lipid thickness, d_l, measured by the gravimetric analysis. This result is in excellent agreement with a similar analysis by Janiak et al., (1979) for dimyristoylphosphatidylcholine bilayers in the gel phase in water. From the values of d_l over the ranges of volume fraction of solvent delimited by the dotted lines in panels A, B, and C of Figure 4, we calculate the area per EPC molecule to be 64.1 ± 1.6 Å^2 (mean ± SD, N = 7 experiments) in water, 70.1 ± 1.0 Å^2 (N = 6) n formamide, and 75.7 ± 2.7 Å^2 (N = 9) in 1,3-PDO. Similar experiments with EPC in glycerol over a similar range of volume fraction of solvent (data not shown) give an average area per molecule of 68.2 ± 3.7 Å^2 (N = 6). For water and formamide, our values for d, d_l, d_s, and area per molecule as a function of volume fraction of solvent are in close agreement to those of Bergenstahl and Stenius (1987).

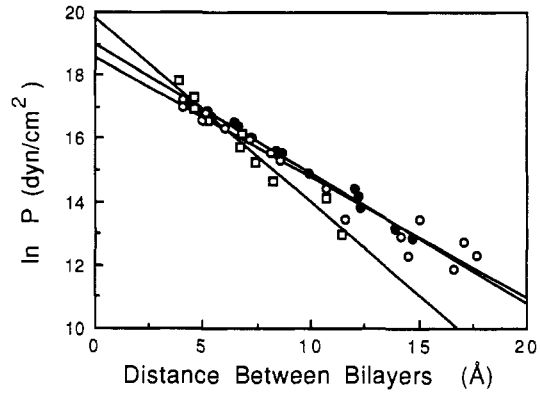

FIGURE 5: Natural logarithm of applied pressure versus distance between adjacent bilayers for EPC multilayers in water (□) [from McIntosh and Simon (1986)], formamide (●), and 1,3-PDO (○).

Both the electron density profiles (Figure 3) and the gravimetric analysis (Figure 4) indicate that the bilayer width remains approximately constant (to within 1–2 Å) over the range of repeat periods in the osmotic stress experiments (Figure 2). This implies that the change in fluid thickness nearly parallels the observed change in repeat period shown in Figure 2. The definition of fluid thickness in the solvation pressure is somewhat arbitrary, as there is as yet no independent method to determine precisely the plane of origin of P_{sol}. Rand, Parsegian, and colleagues (LeNeveu et al., 1977; Lis et al., 1982; Parsegian et al., 1979) have set d_f equal to the partial solvent thickness, d_s, as calculated from eq 3. We (McIntosh & Simon, 1986; McIntosh et al., 1987; Simon et al., 1988) have used the geometric edge of the bilayer as the plane of origin of P_{sol}, since further compression of the lipid lattice results in steric repulsion between the lipid polar headgroups (McIntosh et al., 1987). We have estimated the total width of the bilayer as $d_b = d_{pp}$ + 10 Å, where 10 Å is the approximate width of the EPC headgroup. For the sake of consistency, we use that same definition in this paper. Figure 5 shows plots of ln P versus d_f for EPC in water, formamide, and 1,3-PDO. For all three solvents the pressure decays exponentially with increasing fluid thickness. The lines in Figure 5 are linear regressions to the three sets of data (r^2 > 0.96 for each). Both the intercepts (P_0) and decay lengths (λ) of these lines depend on the solvent molecule (Table III). The decay lengths are 1.7, 2.4, and 2.6 Å for EPC in water, formamide, and 1,3-PDO, respectively. It should be noted that small increases in bilayer thickness upon osmotic compression of the multilayers (within the experimental uncertainty of 1–2

Table III: Decay Length and Magnitude of Solvation Pressure for Bilayers in Three Solvents

solvent	lipid	λ (Å)	V_d (V)	P_0 (dyn/cm^2)	$2\chi(V_d/\lambda)^2$ (dyn/cm^2)
water	EPC	1.7	0.415	4.0×10^8	1.0×10^9
	EPC–Chol	2.1	0.493	3.2×10^8	9.6×10^8
formamide	EPC	2.4	0.266	1.8×10^8	2.2×10^8
	EPC–Chol	2.9	0.353	7.5×10^7	2.6×10^8
1,3-PDO	EPC	2.6	0.223	1.1×10^8	1.3×10^8
	EPC–Chol	3.1	0.292	3.8×10^7	1.5×10^8

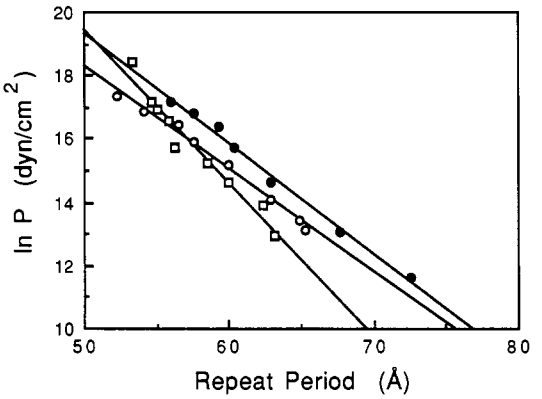

FIGURE 6: Natural logarithm of applied pressure versus lamellar repeat period for EPC–cholesterol multilayers in water (□) [from McIntosh et al. (1989a)], formamide (●), and 1,3-PDO (○).

Å) would tend to increase the values of λ by a few tenths of an angstrom (Simon et al., 1988).

We have performed similar experiments with EPC–cholesterol bilayers. These experiments were of interest since cholesterol has been found to substantially increase the bilayer compressibility modulus (Evans & Needham, 1987), implying that EPC–cholesterol bilayers should have even smaller changes in bilayer thickness upon osmotic compression than EPC bilayers. Figure 6 shows plots of ln P versus d for equimolar EPC–cholesterol bilayers in water, formamide, and 1,3-PDO. Electron density profiles for EPC bilayers in the presence and absence of cholesterol in formamide and 1,3-PDO are shown in panels A and B, respectively, of Figure 7. Similar profiles in water have been published previously (McIntosh et al., 1989a). For each solvent, cholesterol has the effect of increasing the peak-to-peak separation in the electron density profile and raising the electron density of the methylene chain region relative to the geometric center of the bilayer. This is consistent with the localization of cholesterol in the hydrocarbon region of the bilayer, adjacent to the EPC headgroup (McIntosh, 1978). As above, these profiles were used to estimate the total bilayer thickness for EPC–cholesterol bilayers. Plots of ln P versus d_f for equimolar EPC–cholesterol multilayers in water, formamide, and 1,3-PDO are shown in Figure 8. Again, P_{sol} decays exponentially with increasing distance between bilayer surfaces. The straight lines in Figure 8 are linear regressions to the three data sets, each with $r^2 > 0.96$. The measured decay lengths are 2.1, 2.9, and 3.1 Å for EPC–cholesterol bilayers in water, formamide, and 1,3-PDO, respectively (Table III). Also presented in Table III are the magnitudes of the solvation pressure (P_0) for the solvents, obtained by extrapolation of the regression lines to $d_f = 0$.

Dipole potentials were measured to be 266 ± 11 mV (N = 4 experiments), 227 ± 9 mV (N = 5), and 145 ± 7 mV (N = 9) for EPC monolayers on formamide, 1,3-PDO, and glycerol, respectively, and 353 ± 1 mV (N = 3) and 292 ± 5 mV (N = 7) for equimolar EPC–cholesterol monolayers on formamide and 1,3-PDO, respectively (Table III). These dipole potentials can be compared to our previously published (McIntosh et al., 1989a) values of 415 ± 13 mV (N = 3) and 493 ± 13 mV (N = 3) for monolayers over water of EPC and equimolar EPC–cholesterol, respectively.

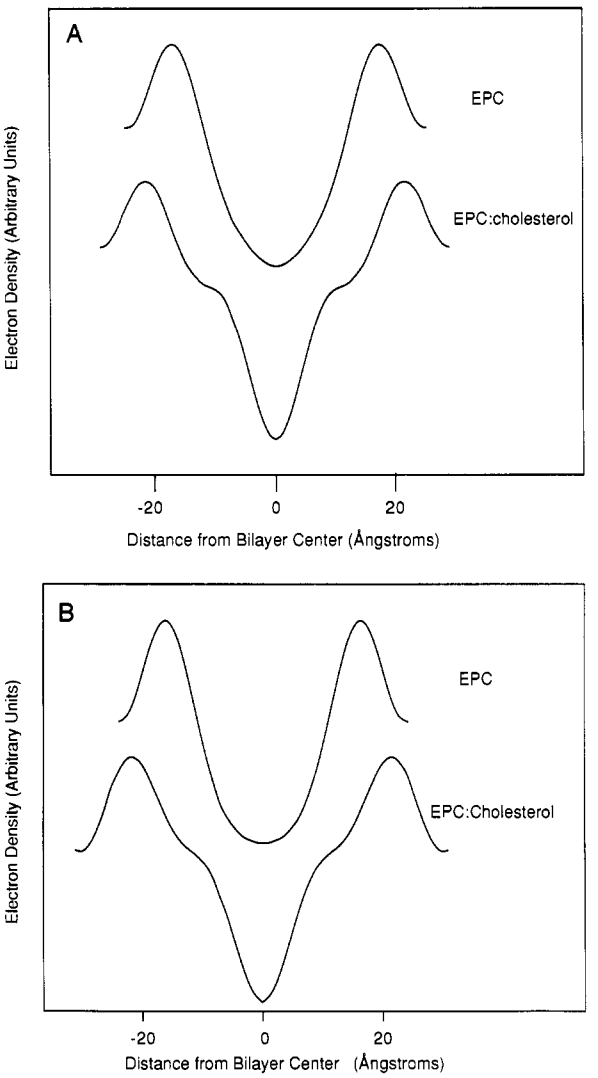

FIGURE 7: Electron density profiles for EPC and equimolar EPC–cholesterol multilayers in (A) formamide and (B) 1,3-PDO.

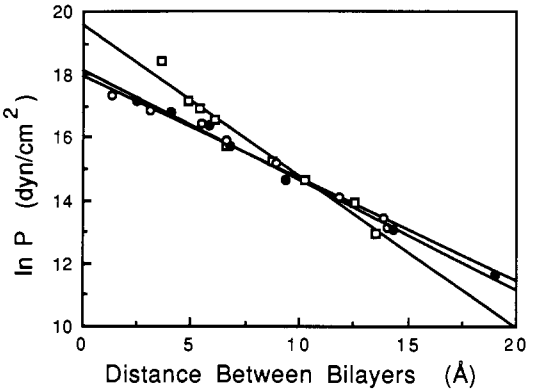

FIGURE 8: Natural logarithm of applied pressure versus distance between adjacent bilayers for EPC–cholesterol multilayers in water (□) [from McIntosh et al. (1989a)], formamide (●), and 1,3-PDO (○).

Discussion

The data presented in this paper provide information on the structure of bilayers and on the interactions between bilayer surfaces in nonaqueous solvents.

Bilayer Structure in Nonaqueous Solvents. The X-ray diffraction experiments show that well-ordered multilamellar liposomes can be formed in the nonaqueous solvents formamide and 1,3-PDO, as well as in water and glycerol. The structure of the bilayer is different in each solvent. The bilayer width, as measured by both electron density profiles Figure 3) and by the Luzzati gravimetric technique (Figure 4), is largest in water and smallest in 1,3-PDO (Table II). Therefore, the area per lipid molecule is largest in 1,3-PDO and smallest in water, with glycerol and formamide having intermediate values (Table I). The relative area per molecule of EPC in all of these solvents can be understood to a first approximation in terms of the different surface tension of the solvents. That is, the area per molecule increases as the surface tension of the solvent decreases. This correlation arises because the energy to expose hydrocarbon to solvent is proportional to the interfacial surface energy, which in general decreases with decreasing solvent surface tension (Israelachvili, 1985). We note that multilamellar liposomes do not form in 1,2-propanediol, a solvent with the same molecular volume as 1,3-propanediol, but a lower surface tension (Table I). This suggests that, when the surface tension is below some critical value, the area per molecule at the lipid/solvent interface increases to the extent that solvent–acyl chain interactions become appreciable and stable liposomes do not form. We note that many lipids are soluble in liquids such as ethanol, methanol, and chloroform, all of which have surface tensions lower than that of 1,2-propanediol.

Although the bilayer thickness and area per lipid molecule depend on the solvent (Tables I and II), the relative changes in thickness and area upon desolvation are similar for EPC in water, formamide, and 1,3-PDO. That is, both the electron density profile analysis (Figure 3) and the gravimetric analysis (Figure 4) indicate that bilayer thickness remains nearly constant (to within 1–2 Å) as the volume fraction of solvent is decreased from about 0.5 to 0.2. The partial lipid thickness and area per lipid molecule were also found to be nearly constant for dioleoylphosphatidylcholine in water and formamide (Bergenstahl & Stenius, 1987).

Effects of Cholesterol on Bilayer Properties. As it does in water, cholesterol increases the bilayer thickness in formamide and 1,3-PDO (Figure 7). This is consistent with cholesterol's ability to decrease the area per EPC acyl chain (Lecuyer & Dervichian, 1969).

As shown in Table III, the magnitude (P_0) and decay length (λ) of the solvation pressure depend on the type of solvent molecule for both EPC and EPC–cholesterol bilayers. For both lipid systems, P_0 and λ vary in a similar manner for the three solvents. That is, for both EPC and equimolar EPC–cholesterol, P_0 is largest in water and smallest in PDO, whereas λ is smallest in water and largest in PDO. The values for λ and P_0 are more secure for equimolar EPC–cholesterol bilayers than for EPC bilayers for two reasons, both of which depend on the lateral compressibility of the bilayer. The first factor is the small deformation of the bilayers as solvent is removed from the multilayers. Our values for λ (Table III) were calculated with the assumption that there was no change in bilayer thickness during solvent removal (see above). A change in bilayer thickness upon desolvation of 1–2 Å would tend to increase λ by a few tenths of an angstrom for EPC bilayers (Simon et al., 1988). The second factor is thermally induced fluctuations in the bilayer, which would tend to decrease λ by a few tenths of an angstrom for EPC bilayers (Evans & Parsegian, 1986). Both of these factors would be smaller if the compressibility modulus of the bilayer were increased (Parsegian et al., 1979; Evans & Parsegian, 1986). The following analysis indicates that the presence of cholesterol increases the compressibility modulus for EPC bilayers in formamide and 1,3-PDO, as well as in water. For 1-stearoyl-2-oleoylphosphatidylcholine (SOPC) bilayers, the incorporation of cholesterol increases the compressibility modulus as measured in water by more than a factor of 5 (Evans & Needham, 1987). Since SOPC has a similar hydrocarbon chain composition to EPC, we assume that cholesterol also comparably increases the compressibility modulus of EPC in water. Since cholesterol orders the hydrocarbon interior of EPC bilayers to a similar extent in formamide (Figure 7A), 1,3-PDO (Figure 7B), and water (McIntosh et al., 1989a), it is expected that cholesterol would also raise the compressibility modulus in formamide and 1,3-PDO. Thus, since for all three solvents the compressibility modulus should be increased upon the incorporation of equimolar cholesterol to EPC bilayers, the deformation upon solvent removal and the thermally induced fluctuations should be reduced by the addition of cholesterol to EPC bilayers. This implies that the EPC–cholesterol data should be more reliable than the EPC data. Therefore, in the following quantitative analysis we use the values of P_0 and λ obtained for EPC–cholesterol bilayers for the three solvents over the same pressure range (Figure 8), although similar arguments could also be made using the data for the EPC bilayers (Figure 5).

For each of the three solvents studied, we obtain a value of λ which is 0.4—0.5 Å larger for EPC–cholesterol than for EPC bilayers (Table III). As discussed above, this difference can be explained by the somewhat larger bilayer deformation upon solvent removal for EPC as compared to EPC–cholesterol bilayers. However, λ may also depend on the lateral structure of the bilayer, as predicted by the recent theoretical analysis of Kornyshev and Leikin (manuscript submitted for publication, personal communication).

Magnitude and Decay Length of Solvation Pressure. An important observation that can be made from the data in Figures 5 and 8 is that the solvation pressure has the same functional form, $P_{sol} = P_0 \exp(-d_f/\lambda)$, for both EPC and equimolar EPC–cholesterol bilayers in three polar solvents. Both the magnitude (P_0) and decay length (λ) of P_{sol} depend on the type of solvent molecule present in the interbilayer space (Table III).

First, let us consider the dependence of λ on the solvent molecule. As noted in the introduction, there have been many different theoretical treatments for the relationship of λ and the solvent. Our data indicate that λ increases with increasing size of the solvent molecule but does not vary monotonically with other properties of the solvent molecule, such as its dielectric constant, index of refraction, or bulk dipole moment (Table I). For example, the dielectric constant of formamide is greater than that of water, whereas the dielectric constant of 1,3-PDO is smaller than that of water. Therefore, we analyze λ in terms of the packing properties of the solvent. Although it is difficult to determine the precise packing arrangement of the solvent molecules in the interbilayer space, measurements of the partial specific volume of water in EPC bilayers (White et al., 1987) suggest that the differences in packing between interbilayer water and bulk water are small. As a first approximation of the packing of solvent molecules in the direction perpendicular to the bilayer surface, we use the cube root of the number of solvent molecules per unit volume ($n_s^{1/3}$) in bulk solution, where $n_s = N_0\rho/M_w$ (N_0 is Avogadro's number, ρ is the solvent density, and M_w is the molecular weight). This calculation makes no assumptions about the shapes of the solvent molecules. In Figure 9, we

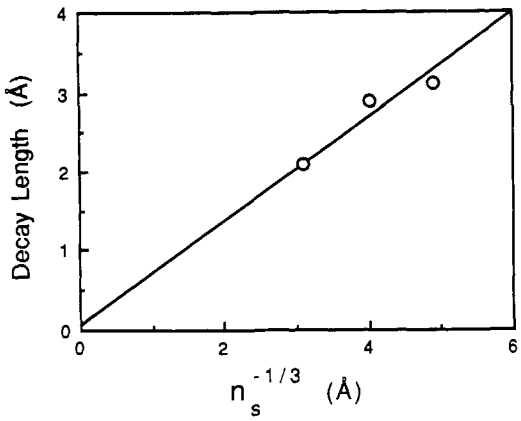

FIGURE 9: Decay length plotted versus the inverse of the cube root of the number of solvent molecules per unit volume.

plot for EPC–cholesterol in water, formamide, and 1,3-PDO the decay length versus $1/n_s^{1/3}$. The straight line in this graph, which has a slope of 0.66, is the least-squares fit ($r^2 = 0.99$) to the three data points plus a point at the origin. The point at the origin was included in the regression since, if we assume that λ does depend on the solvent's dimensions, then λ should approach zero in the limit of a vanishingly small solvent molecule. As can be seen, the three data points fall quite closely to this straight line. This leads to the prediction that the relation between λ and the size of the solvent molecule is $\lambda = 0.66n_s^{-1/3}$. The factor of 0.66 might represent a measure of the packing distribution of the solvent molecules in the interbilayer space. For example, consider the case where the solvent molecules are spherical and hexagonally close packed. In that case, the volume of the solvent molecule may be written $(4/3)(\pi r^3) = 0.74(M_w)/N_0\rho$ (Israelachvili, 1985), where r is the radius of the solvent molecule and the value of 0.74 represents the fraction of volume occupied by matter. Thus, under these conditions $r = 0.56n_s^{-1/3}$, which is similar to our experimental result of $\lambda = 0.66n_s^{-1/3}$. This implies that the decay length, at least for the three solvents studied in this paper, is approximately equal to the "radius" of the solvent molecule calculated by assuming spherical symmetry and hexagonal close packing of the solvent molecules.

As the data in Table III indicate, the magnitude of the solvation pressure (P_0) for three solvents, obtained by extrapolation of P_{sol} to $d_f = 0$, tracks the dipole potential measured for lipid monolayers (in equilibrium with bilayers) over the appropriate solvent. Cevc and Marsh (1985) have developed a theory for the magnitude of P_0 which predicts that $P_0 = 2\chi(\psi/\lambda)^2$, where χ is the orientational susceptibility and ψ is the "hydration potential". In previous studies with aqueous systems, where the dipole potential (V_d) was varied either by changing the area per lipid molecule (Simon et al., 1988) or by changing the lipid headgroups (McIntosh et al., 1989a,b), we have found experimentally that the measured dipole potential provides a good estimate for the value of the hydration potential. Thus, we would expect that $P_0 = 2\chi(V_d/\lambda)^2$, now identifying the dipole potential with the "solvation potential". The observed values of P_0 and those calculated from this expression are presented in Table III. Both the observed and calculated values are largest for lipids in water and smallest for lipids in 1,3-PDO. Also, for both lipid systems for all solvent, the observed and calculated values are within a factor of 4 of each other. Considering the uncertainity in specifying the position of $d_f = 0$, we consider this agreement between prediction and observation to be quite reasonable.

Bilayer Separation in the Absence of Applied Pressure. Finally, we consider the question of why, in the absence of applied pressure, EPC bilayers swell indefinitely in formamide (Figure 4B) and 1,3-PDO (Figure 4C) whereas they imbibe only about 35% water before an excess water phase forms (Figure 4A). This difference in swelling behavior could arise as a result of either larger repulsive pressures between bilayers in formamide and 1,3-PDO than in water or else smaller attractive pressures between bilayers in formamide and 1,3-PDO than in water. The following arguments indicate that *both* factors may contribute. First, for bilayer separations of around 15 Å, where the excess water phase forms, P_{sol} is somewhat greater in formamide and 1,3-PDO than in water (Figure 5). This is because the decay length is larger for the nonaqueous solvents (Table III), so that P_{sol} has a longer range in formamide and 1,3-PDO than in water. Second, the attractive van der Waals pressure might be expected to be smaller for bilayers in formamide and 1,3-PDO as compared to water because of a reduced Hamaker constant, H. The van der Waals pressure can be approximated by $P_v = -H/6\pi d_f^3$. From the Lifshitz formulation (Parsegian & Ninham, 1970) the Hamaker constant for two identical bilayers acting across a fluid medium can be written (Israelachvili, 1985)

$$H \cong \frac{3kT}{4}\left(\frac{\epsilon_b - \epsilon_f}{\epsilon_b + \epsilon_f}\right)^2 + \frac{3h\nu_e}{16\sqrt{2}}\frac{(n_b^2 - n_f^2)^2}{(n_b^2 + n_f^2)^{3/2}} \qquad (5)$$

where $h\nu_e$ is the ionization energy of the bilayer (about 2×10^{-11} ergs), ϵ's are the static dielectric constants, and n's are the indices of refraction, where the subscripts b and f refer to the bilayer and fluid phases, respectively. The first term in eq 5 is the zero-frequency (or static) term and the second term is the higher frequency contribution. The dielectric constants and indices of refraction for water, formamide, and 1,3-PDO are given in Table I. For lipid bilayers, the dielectric constant would be expected to be about 2 and the index of refraction is about 1.45 (Cherry & Chapman, 1967, 1969). Although the use of bulk values of the dielectric constants is problematical, since the polar headgroups may also contribute to the attractive interactions between membranes (Attard et al., 1988), these values can be used to estimate the effects of different solvents on the van der Waals pressure. From eq 5, it can be seen that substitution of formamide or 1,3-PDO for water would have only small effects on the zero-frequency term—formamide would increase this term by about 4% whereas 1,3-PDO would decrease it by about 10%. However, the higher frequency term is much more sensitive to the solvent (McDaniel et al., 1983). That is, since the bilayer index of refraction closely matches that of either formamide or 1,3-PDO, the higher frequency term is much smaller for bilayers in these solvents than in water. Since in the approximation given in eq 5 the higher frequency term accounts for about half of the magnitude of H in water (Mahanty & Ninham, 1976), the substitution of either formamide or 1,3-PDO for water should reduce the magnitude of van der Waals attraction between bilayers by roughly half.

Summary. The pressure–distance relations have been determined for EPC and 1:1 EPC–cholesterol bilayers in water and two nonaqueous solvents. The solvation pressure decays with bilayer separation as a single exponential in all six systems. The decay length depends on the volume density of solvent molecules, whereas the magnitude of the solvation pressure is proportional to the square of the dipole potential as measured in monolayers of these lipids over the appropriate solvent.

ACKNOWLEDGMENTS

We thank Vivian Fowler for an excellent job of typing the

manuscript and Dr. J. M. Corless for the use of his constant-temperature chamber.

Registry No. 1,3-PDO, 504-63-2; cholesterol, 57-88-5; formamide, 75-12-7; water, 7732-18-5.

References

Attard, P., & Batchelor, M. T. (1988) *Chem. Phys. Lett. 149*, 206–211.

Attard, P., Mitchell, D. J., & Ninham, B. W. (1988) *Biophys. J. 53*, 457–460.

Belaya, M. L., Feigelman, M. V., & Levadny, V. G. (1986) *Chem. Phys. Lett. 126*, 361–364.

Bergenstahl, B. A., & Stenius, P. (1987) *J. Phys. Chem. 91*, 5944–5948.

Blaurock, A. E., & Worthington, C. R. (1966) *Biophys. J. 9*, 305–312.

Cevc, G., & Marsh, D. (1985) *Biophys. J. 47*, 21–32.

Cherry, R. J., & Chapman, D. (1967) *J. Mol. Biol. 30*, 551–553.

Cherry, R. J., & Chapman, D. (1969) *J. Mol. Biol. 40*, 19–32.

Christenson, H. K., Horn, R. G., & Israelachvili, J. N. (1982) *J. Colloid Interface Sci. 88*, 79–88.

Crowe, L. M., & Crowe, J. H. (1988) *Biochim. Biophys. Acta 946*, 193–201.

Dean, J. A., Ed. (1985) *Lange's Handbook of Chemistry*, 13th ed., McGraw-Hill Book Co., New York.

Dzhavakhidze, P. G., Kornyshev, A. A., & Levadny, V. G. (1986) *Phys. Lett. A 118*, 203–208.

Evans, B. F., Kolor, E. W., & Benton, W. J. (1983) *J. Phys. Chem. 87*, 533–591.

Evans, E., & Needham, D. (1987) *J. Phys. Chem. 91*, 4219–4228.

Evans, E. A., & Parsegian, V. A. (1986) *Proc. Natl. Acad. Sci. U.S.A. 83*, 7132–7136.

Graham, I. S., Georgallas, A., & Zuckermann, M. J. (1986) *J. Chem. Phys. 85*, 6010–6021.

Gruen, D. W. R., & Marcelja, S. (1983) *J. Chem. Soc., Faraday Trans. 2 79*, 225–242.

Herbette, L., Marquardt, J., Scarpa, A., & Blasie, J. K. (1977) *Biophys. J. 20*, 245–272.

Israelachvili, J. N. (1985) *Intermolecular and Surface Forces*, Academic Press, London.

Israelachvili, J. N., & Pashley, R. M. (1983) *Nature 306*, 249–250.

Janiak, M. J., Small, D. M., & Shipley, G. G. (1979) *J. Biol. Chem. 254*, 6068–6078.

Jonsson, B., & Wennerstrom, H. (1983) *J. Chem. Soc., Faraday Trans 2 79*, 19–35.

Korynshev, A. A. (1986) *J. Electroanal. Chem. 204*, 79–84.

Kwok, R., & Evans, E. (1981) *Biophys. J. 35*, 637–652.

Lecuyer, H., & Dervichian, D. G. (1969) *J. Mol. Biol. 45*, 39–57.

LeNeveu, D. M., Rand, R. P., Parsegian, V. A., & Gingell, D. (1977) *Biophys. J. 18*, 209–230.

Lis, L. J., McAlister, M., Fuller, N., Rand, R. P., & Parsegian, V. A. (1982) *Biophys. J. 37*, 657–666.

Luzzati, V. (1968) in *Biological Membranes* (Chapman, D., Ed.) pp 71–123, Academic Press, New York.

MacDonald, R. C., & Simon, S. A. (1987) *Proc. Natl. Acad. Sci. U.S.A. 84*, 4089–4094.

Mahanty, J., & Ninham, B. W. (1976) *Dispersion Forces*, Academic Press, New York.

Marcelja, S., & Radic, N. (1976) *Chem. Phys. Lett. 42*, 129–130.

McDaniel, R. V., McIntosh, T. J., & Simon, S. A. (1983) *Biochim. Biophys. Acta 731*, 97–108.

McIntosh, T. J. (1978) *Biochim. Biophys. Acta 513*, 43–58.

McIntosh, T. J., & Simon, S. A. (1986) *Biochemistry 25*, 4058–4066.

McIntosh, T. J., & Holloway, P. W. (1987) *Biochemistry 26*, 1783–1788.

McIntosh, T. J., Magid, A. D., & Simon, S. A. (1987) *Biochemistry 26*, 7325–7332.

McIntosh, T. J., Magid, A. D., & Simon, S. A. (1989a) *Biochemistry 28*, 17–25.

McIntosh, T. J., Magid, A. D., & Simon, S. A. (1989b) *Biophys. J. 55*, 897–904.

Nakanishi, K., Matsumoto, T., & Hayatsu, M. (1971) *J. Chem. Eng. Data 16*, 44–45.

Parsegian, V. A., & Ninham, B. W. (1970) *Biophys. J. 10*, 664–674.

Parsegian, V. A., Fuller, N., & Rand, R. P. (1979) *Proc. Natl. Acad. Sci. U.S.A. 76*, 2750–2754.

Parsegian, V. A, Rand, R. P., Fuller, N. L., & Rau, R. C. (1986) *Methods Enzymol. 127*, 400–416.

Persson, P. K. T., & Bergenstahl, B. A. (1985) *Biophys. J. 47*,743–746.

Rand, R. P., Fuller, N. L., & Lis, L. J. (1979) *Nature 279*, 258–260.

Schiby, D., & Ruckenstein, E. (1983) *Chem. Phys. Lett. 95*, 435–438.

Simon, S. A., McIntosh, T. J., & Magid, A. D. (1988) *J. Colloid Interface Sci. 126*, 74–83.

Small, D. M. (1967) *J. Lipid Res. 8*, 551–557.

Tardieu, A., Luzzati, V., & Reman, F. C. (1973) *J. Mol. Biol. 75*, 711–733.

Vink, H. (1971) *Eur. Polym. J. 7*, 1411–1419.

Weast, R. R. C. (1984) CRC Handbook of Chemistry and Physics, 65th ed., CRC Press, Boca Raton, FL.

White, S. H., Jacobs, R. E., & King, G. I. (1987) *Biophys. J. 52*, 663–666.